MICHIGAN STATE
UNIVERSITY

National Superconducting Cyclotron Laboratory

PARTICLE-CORE COUPLING AROUND ^{68}NI: A STUDY OF THE SUBSHELL CLOSURE AT N = 40

A.M. OROS-PEUSQUENS and P.F. MANTICA

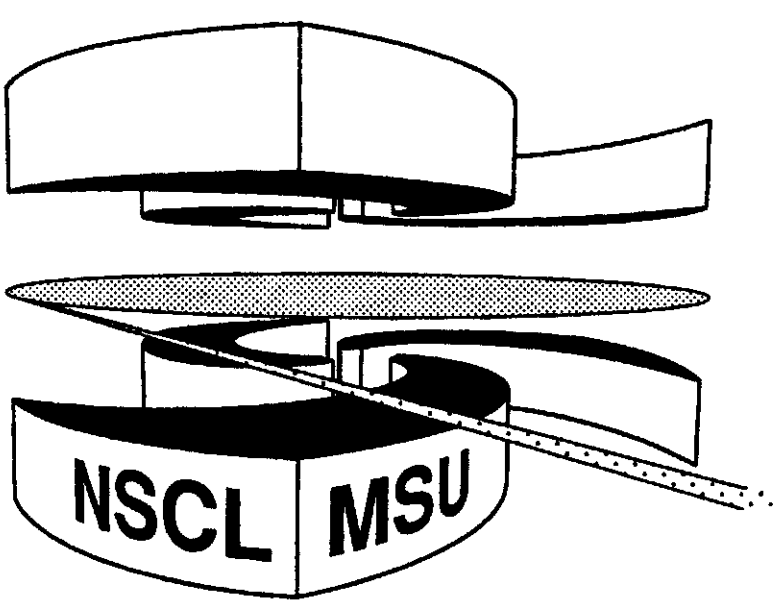

MSUCL-1142

DECEMBER 1999

Particle-Core Coupling around ^{68}Ni: a study of the subshell closure at N=40

A.M. Oros-Peusquens [1*†] and P.F. Mantica [1,2]

[1] *National Superconducting* Cyclotron Laboratory, Michigan *State University,* East *Lansing, MI 48824*

[2] Department of Chemistry, Michigan State University, East Lansing, MI *48824*

Abstract

The existence, of a subshell gap at neutron number N=40 is investigated in the odd-mass Ni and Cu isotopes using the Particle-Core Coupling Model (PCM). The calculated properties are in good agreement with the existing experimental data, suggesting that ^{68}Ni is a good core for the adjacent nuclei. Evaluation of the 2_1^+ excitation energies, two-neutron separation energies, and pairing properties of the Ni isotopes reveals discontinuities at neutron number N=40. These data support the existence of a significant neutron subshell gap at N=40, for Z=28. The systematic behavior of the proton single-particle energies extracted from the particle-core coupling calculations for the odd-mass Cu isotopes is discussed in terms of monopole shifts. The effect is consistent with the existence of a neutron subshell gap at N=40.

PACS:

---

†Corresponding author

*Permanent address: Institute of Nuclear Physics and Engineering Horia Hulubei, Bucharest-Măgurele, Romania

Keywords: NUCLEAR STRUCTURE: BCS, Particle-Core Coupling Model; $^{65-73}$Cu, ^{67,69}Ni calculated levels, electromagnetic properties.

I. INTRODUCTION

A large part of the effects present in the nuclear many-body system seems to be accountable within a shell-model approach. This fact, and the shell structure of the one-body excitation spectrum (the existence of magic numbers), are what make the nuclear many-body system approximately tractable beyond the very lightest nuclei. Knowledge of the evolution of the shell structure with exotic combinations of the neutron and proton numbers, as can be gained from the study of double-closed shell nuclei far from stability, is particularly important in this context. The most neutron-rich double magic nucleus accessible for spectroscopic studies in the near future is ^{78}Ni. The first observation of ^{78}Ni has been reported [1], but spectroscopic information has been obtained only up to ^{70}Ni [2]. The limited amount of information available for the heavy Ni isotopes is due to experimental difficulties in producing neutron-rich nuclei in this mass region.

Perhaps the most exciting phenomenon identified to date in the neutron-rich Ni isotopes is the indication for a subshell closure at N=40 in ^{68}Ni. This was suggested from early transfer studies [3] and reinforced by the observation [4] of a high excitation energy of the first 2^+ state and a pronounced similarity with the excitation spectrum of ^{90}Zr. Although ^{68}Ni is only modestly far from stability (the last stable Ni isotope has A=64), understanding the properties of the nuclei around ^{68}Ni is one important step towards understanding the structure of the more exotic ^{78}Ni. In addition, the existence of a good subshell closure at N=40 is expected to have a significant impact on the properties of the nuclei in the region. The collectivity of the nuclear system is known to be largest when the number of valence nucleons is maximal, which occurs at midshell. A large open shell (in this case N=28–50) can give rise to a large degree of collectivity. On the other hand, the splitting of the shell into two subshells (N=28–40 and N=40–50) can inhibit the development of collective properties.

There is further significance associated with the study of the subshell gap in ^{68}Ni. The single-particle spectrum of nuclei with large neutron excess is predicted by some approaches [5] to become similar to that of a harmonic oscillator with a spin-orbit term (no additional

$\vec{l}^2$ term) and thus reinforce some of the harmonic oscillator magic numbers, as is the case of N=40. A good subshell closure at N=40 in ^{68}Ni might develop into a real shell closure for nuclei with smaller proton numbers. Pursuing the evolution of the N=40 subshell gap in the very neutron-rich nuclei towards ^{60}Ca, while being a very difficult experimental task, would give rich information about the evolution of the nuclear spin-orbit term for large neutron excess.

This paper investigates the low-energy properties of nuclei in the vicinity of N=40, Z=28. First, we examine the empirical evidence for a subshell closure at N=40. The subsequent section concentrates on a Particle-Core Coupling Model (PCM) study of several odd-mass Ni and Cu isotopes. The influence of the subshell closure at N=40 on nuclei adjacent to ^{68}Ni is investigated. From the comparison between the experimental and calculated energies, the proton and neutron single-particle energies are extracted. The behavior of specific proton single-particle energies with mass number is explained in terms of a monopole shift, and supports the existence of an N=40 subshell closure as well.

II. EMPIRICAL EVIDENCE FOR A SUBSHELL CLOSURE AT N=40

The presence of a shell gap in the single-particle spectrum gives rise to "discontinuities" in several properties for the nucleus with the closed shell, as compared to the neighboring nuclei. We have examined several possible indications for a subshell gap in the case of ^{68}Ni.

A. E(2_1^+)

As pointed out by Broda et al. [4], the excitation energy of the first excited 2^+ state E(2_1^+) rises by more than 500 keV between ^{66}Ni and ^{68}Ni. This is a strong indication of an N=40 subshell closure, and also the most pronounced empirical evidence in its favor. The information has been completed with the recent observation [2] of an excitation energy E(2_1^+) in ^{70}Ni very similar to that of ^{66}Ni. The relevant data are summarized in Fig. 1.

On the other hand, the behavior of the $E(2_1^+)$ values in the even Zn (Z=30) and Fe (Z=26) isotopes, shown for comparison in Fig. 1, is intriguing. A clear difference in $E(2_1^+)$ can be observed for N=40, as compared to N=38, but this time the energy is lower than the one of the preceding nucleus. Nevertheless, the first excited 2^+ state in the "two-proton particle" Zn or "two-proton hole" Fe isotopes is expected to be of predominant proton nature. The effect of, for example, changes in the proton single-particle energies on the excitation of the 2_1^+ state cannot be easily disentangled from the effect of the neutron subshell closure on the same state.

B. S(2n)

A pronounced drop in the two-neutron separation energies S_{2n} is expected immediately *after* a neutron shell closure. The effect of a *subshell* closure on the S_{2n} values is less pronounced, and mainly gives rise to a change of the slope of the separation energies. A more sensitive quantity is the derivative of S_{2n} as a function of mass. The behavior of the derivative is reflected by the differential quantity $S_{2n}(A)$-$S_{2n}(A+2)$. The differential two-neutron separation energies of the Ni isotopes are shown in Fig. 2(a). For comparison, the similar quantity calculated from the two-proton separation energies is shown in Fig. 2(b) for the N=50 isotones, which cross the Z=40 subshell closure in ^{90}Zr. The two-neutron and two-proton separation energies are taken from the evaluation of Ref. [8]. Similar effects can be noticed at the crossing of N=40 in the Ni isotopes, as at the crossing of Z=40 in the N=50 isotones. The magnitude of the effect is larger in the N=50 isotones, but this might be due to a somewhat different single-particle spectrum, giving rise to an additional gap between the pair of orbitals $2p_{3/2}$, $1f_{5/2}$ and the orbital $2p_{1/2}$, as well as additional binding of ^{88}Sr.

The errors on the adopted separation energies become very large just in the region of interest for ^{68}Ni. Additional effort for precise mass measurements may provide a clear signature for subshell effects at N=40.

C. Pairing properties

Another quantity which can show discontinuities at the crossing of a shell closure is the pairing gap Δ. A good estimate for the neutron pairing gap from the experimental neutron separation energies is [9]:

$$\Delta_n = -1/4\,\{S_n(N-1,Z) - 2S_n(N,Z) - S_n(N+1,Z)\}\,,$$

for even N values, or the same quantity with opposite sign for odd N values.

The neutron pairing gap in the Ni isotopes, extracted from the adopted S_n values [8], is shown in Fig. 3. A minimum value for the experimental gap is found for ^{68}Ni. Due to the large experimental errors on the separation energies, the errors in Δ_n become large precisely in the interesting region (after ^{68}Ni).

In order to investigate in more detail the information which can be extracted from the experimental pairing gaps, we have calculated this quantity in a standard BCS approach with a constant pairing force. As a starting point,

The neutron single-particle energies from ^{57}Ni were used as a starting point for the Ni isotopes with N>28. The pairing strength was adjusted to reproduce the experimental pairing gap in ^{59}Ni. For the isotopes with N<28, the orbital $1f_{7/2}$ was added, and the pairing strength was determined from the experimental pairing gap in ^{54}Ni. Some variation of the single-particle energies was allowed for the heavier isotopes (N>28), and determined from a best qualitative description of the experimental data. The main result of this study is the fact that the low value of Δ_n in ^{68}Ni cannot be reproduced in the BCS approach, when the single-particle energies and pairing strength from the lighter isotopes are extrapolated to N=40. The discrepancy is visible in Fig. 3, despite the large experimental errors.

Information from both one-neutron stripping and pick-up is available for ^{59,61,63}Ni, and from one-neutron stripping for ^{65}Ni [7]. From comparison of the spectroscopic factors for the same state obtained in stripping and in pick-up, the occupation probability for a given single-particle orbital can be determined. The distribution of neutron particles in the major

shell N=28–50 points toward a substantial subshell gap at N=40. The occupancy of the $1g_{9/2}$ orbital, extracted from experiment, is consistent with zero. Excitations involving orbitals below N=40 can, therefore, be approximated rather well by pure hole excitations. In addition, excitations involving $1g_{9/2}$ can be considered pure particle excitations. This conclusion constitutes the basis of the study of the odd Ni isotopes around ^{68}Ni in the Particle-Core Coupling Model.

III. PARTICLE-CORE COUPLING MODEL CALCULATIONS

A. The model

Several odd-mass and even-even isotopes in the vicinity of ^{68}Ni were studied in the particle-core coupling model (PCM). A detailed description of the model can be found in Refs. [10–12], but we summarize here its main features for completeness.

The model space for the odd-mass nuclei around ^{68}Ni, described herein, consists of single-hole or -particle states coupled to collective quadrupole and octupole vibrational excitations of the underlying even-even core. It is assumed that the core does not change whether a proton or a neutron particle or hole is coupled to it. In addition to the "natural" configuration space consisting of collective excitations in ^{68}Ni coupled to single-hole or single-particle excitations, an additional subspace has been included, which accounts for neutron or proton excitations of the type two-particle one-hole (2p-1h) or one-particle two-hole (1p-2h). This latter part of the model space can be approximated by hole or particle excitations coupled to the collective excitations of $^{68\pm2}$Ni for the odd-neutron Ni isotopes, or of the corresponding Zn isotopes for the odd-proton Cu isotopes.

For each subspace, the hamiltonian includes a single-particle, a collective, and an interaction part:

$$\hat{H} = \sum_j \hat{h}_{\rm sp}(j) + \sum_{\lambda=2,3} \hat{H}_{\rm coll}(\lambda) + \hat{H}_{\rm PVC}. \qquad (1)$$

The different terms of the hamiltonian are:

$$\hat{h}_{\rm sp}(j) = \epsilon_j \, a_j^\dagger \cdot \tilde{a}_j, \tag{2}$$

where ϵ_j is the single-particle energy of a given orbital (nlj), and $a_j^\dagger$, $\tilde{a}_j$ are the creation and annihilation operators for the fermionic (single-particle) excitations,

$$\hat{H}_{\rm coll}(\lambda) = \left(\hat{n}_\lambda + \frac{2\lambda+1}{2}\right)\hbar\omega_\lambda, \tag{3}$$

where $\hat{n}_\lambda$ is the boson number operator, and $\hbar\omega_\lambda$ denotes the energy of the vibrational 2^λ-pole phonon, and

$$\hat{\rm H}_{\rm PVC} = -\sum_{\lambda=2,3} \xi_\lambda \hbar\omega_\lambda \left(\frac{\pi}{2\lambda+1}\right)^{1/2} \frac{r^\lambda}{< r^\lambda >} \sum_{\mu=-\lambda}^{\lambda} [b_{\lambda\mu}^\dagger + (-)^\mu b_{\lambda-\mu}] Y_{\lambda\mu}^*(\hat{r}), \tag{4}$$

where ξ_λ gives the strength of the particle-vibration coupling of multipole λ, $< r^\lambda >$ is the mean value of the radial integral for the orbitals in the major shell, and $b_{\lambda\mu}^\dagger$, $b_{\lambda-\mu}$ are the creation and annihilation operators for the bosonic (collective phonons) excitations. The coupling of the two subspaces is treated in the manner described in Ref. [13].

Taking as an example the case of ^{67}Ni, the neutron-hole orbitals $2p_{3/2}^{-1}$, $1f_{5/2}^{-1}$ and $2p_{1/2}^{-1}$, as well as the deep hole states $1f_{7/2}^{-1}$, $1d_{3/2}^{-1}$ and $2s_{1/2}^{-1}$ are considered in the "^{68}Ni-subspace". For the neutron 1p-2h excitations in the "^{66}Ni-subspace", we take into account the orbitals $1g_{9/2}$, $2d_{5/2}$ and $1g_{7/2}$ above N=40. For the proton case, the proton-particle orbitals are $2p_{3/2}$, $1f_{5/2}$, $2p_{1/2}$ and $1g_{9/2}$; for the proton-hole orbitals we include $1f_{7/2}^{-1}$ as well as $2s_{1/2}^{-1}$, $1d_{3/2}^{-1}$ and $1d_{5/2}^{-1}$. The need to include deep hole states for the description of odd-Z nuclei around ^{68}Ni is clear from the experimental structure of ^{63}Co, where large fragments of the $\pi 2s_{1/2}^{-1}$ and $\pi 2d_{3/2}^{-1}$ hole orbitals are found around 2.5 MeV [7,14,15]. We have included the corresponding neutron deep-hole states in the description of the odd-neutron Ni isotopes for consistency, but their energy cannot be reliably determined from the existing data.

The collective configurations taken into account in the calculations include up to three quadrupole phonons and two octupole phonons. For mixed quadrupole-octupole multiphonon states, only the one quadrupole-one octupole multiplet has been included. Anharmonicities are considered by allowing for non-zero mass quadrupole moments of the quadrupole and octupole phonons [12,16]. This approach leads to quadrupole-quadrupole

diagonal terms which remove the degeneracy in the multiphonon spectrum as well as in the particle(hole)-phonon multiplets. The quadrupole moments of the single-particle orbitals are calculated using the wave functions obtained with the Woods-Saxon potential with the parameters of Ref. [17]. Because of the large magnitude of the coupling constant involved in the diagonal quadrupole-quadrupole hamiltonian [16], $\kappa_2 = -6.2\ 10^{-3}$ MeV fm^{-4} (for comparison, $\kappa_2 = -0.46\ 10^{-3}$ MeV fm^{-4} in ^{208}Pb), and the non-negligible quadrupole moments involved, the effects of the quadrupole-quadrupole splitting within the particle- or hole-phonon or phonon-phonon multiplets are large (several hundreds keV).

No microscopic structure of the phonons is taken into account, and, consequently, the effects of the Pauli principle on the properties of states of the type phonon $\otimes$ hole or particle cannot be accounted for.

One important aspect to be considered is related to the overly-simplified description of the even-even core in terms of anharmonic vibrational states. In the case of ^{68}Ni, the first excited state has $J^\pi = 0^+$ and lies nearly 300 keV below the 2_1^+ state supposed to be the quadrupole shape vibration. This 0^+ state is clearly not included in the model space, but it may give rise to low-energy excitations in the neighboring odd nuclei. Another excitation of ^{68}Ni which may play an important role in the sequence of levels observed in the odd-mass nuclei is the 5_1^- isomeric state at 2847 keV, with a probable shell model configuration $\nu 1g_{9/2}\nu 2p_{1/2}^{-1}$. The 5_1^- state of the PCM is a two-phonon ($2^+ \otimes 3^-$) excitation, and too high in energy to correspond to the experimentally observed isomer. For ^{70}Ni, the 6_1^+ and 8_1^+ states (the latter being an isomeric state with $T_{1/2}$=0.21(5)μs) are predominantly of two-particle $\nu 1g_{9/2}^2$ character, and a three- or four-phonon approximation cannot be used for the description of these states. The influence of these configurations on the experimental spectra will be discussed later for specific cases.

B. Results

The aim of the particle-core coupling study presented in this section was twofold: (i) investigating if ^{68}Ni is a good core for the adjacent nuclei; and (ii) extracting information about the neutron and proton single-particle energies around N=40, Z=28.

Shell model studies have been performed in this region for the Ni, Cu and Zn isotopes [2,4,18–23]. A few Ni and Zn isotopes have been studied in the framework of a microscopic model based on Hartree-Fock-Bogoliubov theory [24,25]. QRPA calculations of half-lives and Gamow-Teller decay properties are available for a number of nuclei in this region (see Ref. [26]). Despite the large number of studies, the present understanding of the region is far from complete. The shell model calculations give a fair description of the general aspects met around ^{68}Ni. Due to necessary restrictions on the configuration space, proton excitations across the Z=28 shell gap are not taken into account. An important class of excitations is thus excluded. Examples of low-energy and near-yrast states poorly reproduced by the shell model calculations have been found (see, for example, Ref. [21]).

The particle-core coupling model gives an interesting alternative to the shell model calculations. Excitations across the shell closure at Z=28 (and subshell closure at N=40) can be accounted for. The parameters of the model have a clear physical interpretation and, once they are extracted from the comparison of the calculated levels with the experimental data, give important information about the core (collectivity of the phonon excitations, quadrupole moments) and the odd nucleus ("bare" single-particle energies). However, determining the best values for the model parameters requires unambiguous experimental data for nuclei in the region under study. Since non-collective states in the core nuclei are not adequately described, the corresponding configurations in the odd nuclei are also missing from the model space.

The parameters used in the calculations for odd-mass nuclei around ^{68}Ni are summarized in Tables I and II. The results of the calculations are discussed in detail in the next subsection.

Since the model parameters are determined from the available experimental data, and do change with mass number, the predictive power of the model for nuclei where no data exist is limited. It cannot be overly emphasized that the results are only as good as the data used to determine the parameters of the model. On the other hand, once these parameters have been reliably determined, the descriptive power of the model is high.

1. Odd-A Ni isotopes

The energy levels of the odd-A Ni isotopes in the immediate vicinity of ^{68}Ni can provide evidence for a significant subshell closure at ^{68}Ni. For an open shell odd-mass nucleus A, an average core composed from the even-even A-1 and A+1 nuclei would be needed. In the case of a strong subshell closure, distinct excitations corresponding to a dominating ^{68}Ni core should exist in the odd-neutron nuclei.

The known experimental levels of ^{67}Ni [7,19,24,26,27] and ^{69}Ni [2,28,29,23,30] are shown in Fig. 4, along with the levels calculated in the particle-core model and selected experimental states in the core ^{68}Ni. The calculated single-particle strength in ^{67,69}Ni is shown in Fig. 5.

^{67}Ni

The calculated structure of ^{67}Ni is rather simple. Predominant 1h character is found for the low-energy negative parity levels $(1/2^-_1)$ g.s., $(5/2)^-_1$, and, to a lesser extent, for $(3/2)^-_1$ (see fig. 5). The higher-energy negative-parity $(5/2^-)$ state observed in β decay is a member of the quadrupole doublet $2^+ \otimes p^{-1}_{1/2}$. As noted in Ref. [30], the population of the $(5/2^-)$ state at 2155 keV in β decay from the $(7/2^-)$ g.s. of ^{67}Co [26], is probably due to a small neutron-hole component $1f^{-1}_{5/2}$ in its structure. The ratio of the calculated spectroscopic factors for $5/2^-_2$ and $5/2^-_1$, given in Fig. 5, is consistent with the relative $\log ft$ values from β decay. We stress that the excitation energy of the $5/2^-_2$ state, close to that of the 2^+_1 state in ^{68}Ni, shows that the description of ^{67}Ni in terms of a dominant ^{68}Ni core plus one hole is correct. A core averaging ^{66}Ni and ^{68}Ni will give a substantially lower $5/2^-$ state, with a

rather large spectroscopic factor and low $\log ft$ in $\beta-$decay.

The calculated $9/2^+$ state at 1.013 MeV is the lowest 2p-1h excitation in ^{67}Ni. The lowering from the unperturbed energy $E_u = \epsilon(1g_{9/2}) - \epsilon(2p_{1/2})$, which gives the subshell gap at N=40, is due to the gain in pairing energy (one additional pair in the 2h-1p states compared to the 1h states) and to the stronger coupling in this "second subspace" (^{66}Ni+1p). The summed effects could account for a lowering of approximately 2 MeV from the unperturbed position, and thus reflect a substantial N=40 gap.

^{69}Ni

The low-energy structure of ^{69}Ni has been recently deduced from isomeric decay [2,30] and $\beta-$decay [23] studies. The level at 2241 keV was observed by Grzywacz et al. [2] to $\gamma-$decay to the $(9/2^+)$ ground state and tentatively assigned as $(13/2^+)$. The decay mode indicates a possible structure $2^+(^{68}\text{Ni})\otimes\nu 1g_{9/2}$ for this state. Considering a dominant ^{68}Ni core, the $2^+(^{68}\text{Ni})\otimes\nu 1g_{9/2}$ multiplet should cluster around the energy of the core 2^+ state (2033 keV). From the particle-core model study of ^{69}Cu (see following subsection), a small and negative mass quadrupole moment is derived for the first 2^+ state of ^{68}Ni. Using this negative value of $Q(2^+)$, the model predicts states having spin and parity $11/2^+$ or $9/2^+$ near the experimental level at 2241 keV, whereas the $13/2^+$ state of the quadrupole multiplet is predicted $\sim$400 keV lower in energy. The feeding and decay of the level at 2241 keV is consistent with either $13/2^+$ or $11/2^+$ spin and parity assignment.

The experimental observation of a state with probable $2^+(^{68}\text{Ni})\otimes\nu 1g_{9/2}$ character at approximately the energy of the ^{68}Ni core 2^+ energy again provides strong support for a dominant ^{68}Ni core.

In addition to states of ^{68}Ni$\otimes$particle character, a number of negative-parity levels in ^{69}Ni probably belong to the ^{70}Ni$\otimes$hole subspace. The high density and low energy of these levels can be attributed to the stronger particle-vibration coupling and lower energy of the 2_1^+ state in the subspace of ^{70}Ni, and the higher density of single-hole, as compared to single-particle, orbitals. The $(17/2^-)$ isomer observed by Grzywacz et al. [2], and most of the levels populated in its subsequent $\gamma-$decay most likely belong to this second subspace,

as discussed by Mueller et al. [23]. The probable origin of the $(17/2^-)$ state is $8^+_1 \otimes \nu 2p^{-1}_{1/2}$, where 8^+_1 is the isomeric state observed in ^{70}Ni [2], and the $(13/2^-)$ state is 6^+_1 (^{70}Ni$\otimes\nu 2p^{-1}_{1/2}$). The two core states, and the corresponding $(17/2^-)$ and $(13/2^-)$ states in ^{69}Ni are outside the configuration space of the PCM, but the lower spin, negative parity states are well reproduced. Population of the $(5/2^-)$ states via Gamow-Teller $\beta-$decay ($\log ft \sim 5$) of the $(7/2^-)$ $\pi 1f^{-1}_{7/2}$ ground state of ^{69}Co can be attributed to the calculated $\nu 1f^{-1}_{5/2}$ component in their wave functions (see Fig. 5).

The particle-core model provides an overall good description of the known levels in the odd-mass ^{67,69}Ni isotopes adjacent to ^{68}Ni. In each isotope, a member of the quadrupole multiplet was identified at an energy close to that of 2^+_1 in ^{68}Ni, providing direct evidence that ^{68}Ni is a good core for the two nuclei.

2. Cu isotopes

Extended configuration space

The experimental data we are aiming to describe contain states which probably involve the 0^+_2 and 5^-_1 excitations of the Ni cores, as indicated by structure-selective β decay experiments [31]. We have therefore introduced the 0^+ and 5^- core configurations in the model space. A similar situation is described in Ref. [32] for the case of ^{116}Sn–^{115}In. The coupling of the extra configurations to the vibrational ones was treated as if the 0^+ and 5^- states had two-phonon character, but the coupling strength was reduced as compared to the one used for the phonon states of the model. The energies of the two configurations were taken from experiment, and shifted downwards by the calculated energy lowering of the ground-state of the odd nucleus. This is needed to compensate for basis truncation effects, since higher-lying configurations built on the 0^+ and 5^- states are not included in the model space. Van Isacker et al. [33] pointed out that the coupling of single-particle or -hole excitations to the *vibrational* states of the core is the most important factor in determining the structure of low-lying levels and the fragmentation of the single-particle strength in the odd nuclei. The

particle⊗vibration subspace was found [33] to be nearly orthogonal on the particle⊗(non-collective excitations). We do not expect the non-collective configurations included in the model to renormalize the model parameters. For example, we use for the calculations on ^{69}Cu the same core parameters used for ^{67}Ni and ^{69}Ni. Nevertheless, when configurations of the two different types come close in energy, even a reduced interaction can lead to a significant mixing.

We have used this extended configuration space for the odd-mass Cu isotopes with N≥40. The experimental levels for ^{69}Cu, ^{71}Cu and ^{73}Cu, along with the results of the PCM calculations, are shown in Fig. 6.

^{69}Cu

The single-particle states of ^{69}Cu can be identified from the results of the proton transfer reactions [35,36]. The largest component of the ground-state is $\pi 2p_{3/2}$, the state at 1096 keV is mainly $\pi 2p_{1/2}$, the state at 1213 keV is mainly $\pi 1f_{5/2}$, and the two $(7/2^-)$ states at 1711 keV and 1871 keV share a rather large $\pi 1f_{7/2}^{-1}$ strength. The β decay of the 3.4 s, $1/2^-$ isomer, in ^{69}Ni proceeds almost exclusively to a $(3/2^-)$ level at 1296 keV [23,30] and to the ground-state of ^{69}Cu. This pattern has been discussed in detail [23,30], and the $(3/2_2^-)$ level was assigned a neutron two-particle two-hole $\otimes\pi 2p_{3/2}$ structure. Additional excited levels in ^{69}Cu have been observed following the β decay of the $(9/2^+)$, $\nu 1g_{9/2}$ ground-state of ^{69}Ni [27,31,37]. However, only a few states, all above 2.5 MeV, have logft values consistent with an allowed Gamow-Teller transition. From shell model considerations, their most probable microscopic configurations are: $\pi 2p_{3/2}(\nu 1g_{9/2}2p_{1/2}^{-1})$, $\pi 2p_{3/2}(\nu 1g_{9/2}2p_{3/2}^{-1})$ and $\pi 1g_{9/2}$. In the PCM, the corresponding macroscopic configurations are $5^-(^{68}\mathrm{Ni})\otimes\pi 2p_{3/2}$, $3^-(^{68}\mathrm{Ni})\otimes\pi 2p_{3/2}$ and $\pi 1g_{9/2}$, respectively. The isomeric level at 2741 keV, with half-life 0.36(5) μs, has been assigned spin-parity $(13/2^+)$ and probable structure $5^-(^{68}\mathrm{Ni})\otimes\pi 2p_{3/2}$ [2,34,38]. Using the B(E2)-value for ^{68}Ni given in Table III, we calculated for the reduced transition probability for the isomeric decay a value of B(E2; $13/2_1^+ \rightarrow 9/2_1^+$)=5.3 e^2 fm^4, to be compared to the experimental value B(E2; $(13/2_1^+) \rightarrow (9/2_1^+)$)=7.2(1.0) e^2 fm^4.

The results of the PCM calculations for ^{69}Cu are in good agreement with the exper-

imental data. A *negative* quadrupole moment of the 2_1^+ state in the ^{68}Ni core is needed to correctly account for the existence of the two $(7/2_2^-)$ states at 1711 and 1871 keV. The two low-lying $7/2^-$ configurations of the model are $(\pi 2p_{3/2})^2_{0^+}\pi 1f_{7/2}^{-1}$ (2p-1h excitation) and $2_1^+(^{68}\mathrm{Ni})\otimes\pi 2p_{3/2}$.

The existence of a low-lying $(7/2^-)$ state with a significant proton 2p-1h component is worth emphasizing. The spectroscopic factor of the first $7/2^-$ state, measured in one proton pick-up reaction, is S=0.34 [35]. The second $7/2^-$ state, with a dominant $2^+\otimes 2p_{3/2}$ structure, has a small 2p-1h component, S=0.06. An excited "quasi-band" of 2p-1h character, built on the lowest $7/2^-$ state, has been observed by Ishii et al. [34] and is shown in Fig. 6(a). As noted earlier, the particle-core model can account for proton 2p-1h excitations, and describes well the states in ^{69}Cu belonging to this category. In particular, the decay within the "quasi-band" built on the $7/2_1^-$ state is well reproduced (see Table III).

^{71}Cu

The level scheme of ^{71}Cu calculated in the PCM (Fig. 6(b)), shows good agreement with the experimental level scheme, with the exception of the high spin $(19/2^-)$ isomer and the $(15/2^-)$ state. These states most likely arise from the coupling of the $\pi 2p_{3/2}$ orbital to the 8^+ isomeric state at 2860 keV and 6^+ state at 2677 keV in ^{70}Ni [2]. The latter states are not correctly accounted for in the model space, as discussed earlier. Nevertheless, the lower-spin states involved in the decay of the $(19/2^-)$ isomer are well described.

Probable spin-parity $(7/2^-)$ can be inferred for the states at 981 keV and 1189 keV, populated by parallel cascades from the $(19/2^-)$ isomer. The main decay path populates the 1189 keV state, with calculated $2^+(^{70}\mathrm{Ni})\otimes\pi 2p_{3/2}$ dominant component. The dominant structure of the lower $(7/2^-)$ state at 981 keV is a 2p-1h excitation with the hole in the $\pi 1f_{7/2}$ orbital. These structure assignments result from the PCM calculations and are supported by the experimental decay mode. Furthermore, combining the model predictions *and* the experimental data, it is likely that the sequence of levels at 1972 keV, 1452 keV and 981 keV form an $11/2^-$, $9/2^-$, $7/2^-$ "quasi-band" built on the $7/2^-$ state of 2p-1h character. This situation is similar to what is observed in ^{69}Cu. The parallel, stronger cascade from

the $(19/2^-)$ isomer proceeds via states with ^{70}Ni core-coupled configurations.

^{73}Cu

The experimental information concerning excited states in ^{73}Cu stems entirely from the β decay experiment of Franchoo et al. [31]. Very little is known about the spin-parity of the states. The first excited level was assigned $(5/2^-)$ by Franchoo et al. [31], based on its feeding in β decay. The absence of β feeding to the ground-state suggests that ground-state spin-parity $3/2^-$ is maintained. According to Franchoo et al. [31], these two states correspond to the single-particle configurations $\pi 2p_{3/2}$ and $\pi 1f_{5/2}$. No other suggestion is made concerning the spin-parity and structure of the higher-lying levels. The scarce experimental information for ^{73}Cu, as well as for the core ^{72}Ni, did not allow us to uniquely determine the model parameters for ^{73}Cu. We therefore extrapolated the parameters used for ^{69}Cu and ^{71}Cu to ^{73}Cu (see Tables I and II). The levels of ^{73}Cu resulting from the PCM calculations are compared to the experimental levels in Fig. 6(c). Based on the systematics in ^{69}Cu and ^{71}Cu, and on model predictions, we suggest very tentatively spin and parity $7/2^-$ for the levels at 961 keV and 1010 keV. The state at 961 keV, which decays to the ground-state, is a possible candidate for the predicted $2_1^+(^{72}\mathrm{Ni})\otimes\pi 2p_{3/2}$ configuration. The state at 1010 keV decays to the ground-state and first excited state, and is populated in β decay. It may correspond to the lowest 2p-1h excitation in ^{73}Cu. Either of the two states at 1297 and 1489 keV might correspond to the calculated $9/2^-$ state. For the similar states in the lighter Cu isotopes, feeding in β decay from a $(9/2^+)$ parent has been observed. The $9/2^+$ model state, with a large $\pi 1g_{9/2}$ component, should also be populated in the β decay from the $(9/2^+)$ ground state of ^{73}Ni. It might correspond to the remaining level (at 1297 or 1489 keV) seen in β decay.

The extrapolation of the model parameters to ^{73}Cu was based on the trends seen in the lighter isotopes, with the exception of the energy of the lowest 2p-1h excitation. A linear extrapolation of the trend deduced from ^{69}Cu and ^{71}Cu would imply a very low energy for the $7/2^-$ state of 2p-1h character in ^{73}Cu. In such a case, the 2p-1h configuration might become the lowest excited state, or even the ground-state, of ^{73}Cu. Nevertheless, the absence

of β feeding to the ground-state of ^{73}Cu [31] does not support such an assignment. We chose, therefore, to extrapolate the other parameters of the model and fix the energy of the lowest 2p-1h excitation so that it corresponds to the 1010 experimental state.

Summarizing, the properties of the states in the odd-mass Cu isotopes with "regular" structure, i.e. one proton particle coupled to the Ni cores, are well reproduced in the particle-core model. A very interesting aspect observed in the heavy Cu isotopes is the existence of low-lying states based on 2p-1h excitations. A "quasi-band" built on the lowest 2p-1h excitation, with the hole in the $\pi 1f_{7/2}^{-1}$ orbital, has been identified experimentally in ^{69}Cu by Ishii et al. [34] and is well reproduced by the PCM calculations. Based on the model predictions and the experimental level scheme, the existence of a similar "quasi-band" is suggested for ^{71}Cu. The behavior of the lowest 2p-1h states in the neutron-rich, odd-mass Cu isotopes is shown in Fig. 7. The spectroscopic factors measured in the proton pick-up reaction (t,^{3}He) are given where available. A significant lowering of 700 keV of the state with large 2p-1h component (large experimental spectroscopic factor) is noticed between ^{67}Cu and ^{69}Cu. Support for a further lowering of the 2p-1h configuration in ^{71}Cu could be inferred from the available data, based on the results of PCM calculations.

3. Single-particle energies and monopole shifts

The single-particle energies extracted from comparison of the experimental levels with the PCM calculations are listed in Table II. We add to the results already discussed the proton single-particle energies for ^{65}Cu and ^{67}Cu, based on the comparison shown in Fig. 8.

We point out that the values extracted represent "bare" single-particle energies, from which the effect of the dominant quadrupole and octupole terms of the proton-neutron interaction has been removed. The binding energies of the single-particle orbitals in ^{68}Ni are further extracted using the experimental neutron and proton separation energies. The single-particle energies in ^{68}Ni are summarized in Fig. 9 and compared to those for ^{56}Ni, extracted in a very similar manner by Trache et al. [39], and the predictions of Duflo and

Zuker [40], which involve a new parametrization of the nuclear monopole hamiltonian.

The behavior of the proton energies in the odd-mass Cu isotopes with mass number is partially due to mean-field effects, but also to the *monopole* part of the proton-neutron interaction. As discussed by Franchoo et al. [31], the energy spacing between the states with single-particle character $\pi 1f_{5/2}$ and $\pi 2p_{3/2}$ decreases rapidly after N=40. This "monopole shift" has been attributed to the monopole interaction of the proton in the orbital $\pi 1f_{5/2}$ with neutrons in $\nu 1g_{9/2}$, which is stronger than the corresponding interaction when the proton occupies the reference orbital $\pi 2p_{3/2}$. Monopole shifts are observed in other mass regions, for example in the Sb isotopes (migration of the $\pi 1g_{7/2}$ orbital relative to $\pi 2d_{5/2}$ when the neutron orbital $\nu 1h_{11/2}$ gradually fills) and in the N=83 isotones (migration of the $\nu 1h_{9/2}$ orbital relative to $\nu 2f_{7/2}$ after Z=64, when the proton orbital $\pi 1h_{11/2}$ gradually fills). The orbital having the (n, l) quantum numbers closest to those of the filling neutron orbital is mainly influenced by the monopole shift [41].

The monopole shift of the $\pi 1f_{5/2}$ orbital relative to $\pi 2p_{3/2}$ in the heavy Cu isotopes is as pronounced as the drop in the energy of the $(5/2^-)$ state. The $\pi 1f_{5/2}$ single-particle energies needed to reproduce the spectra of ^{69}Cu, ^{71}Cu and ^{73}Cu are 0.9, 0.25 and -0.30, respectively, all energies given relative to that of $\pi 2p_{3/2}$. If this effect is attributed entirely to the occupancy of the $\nu 1g_{9/2}$ orbital, the $\pi 1f_{5/2}$ orbital is expected to be around 2 MeV lower than $\pi 2p_{3/2}$ in ^{78}Ni. As observed experimentally, $\pi 1f_{5/2}$ is indeed the lowest orbital of the Z=28-50 shell in the neutron-rich N=50 isotones (e.g. a $(5/2^-)$ ground-state in ^{81}Ga, ^{83}As and a low-lying $5/2^-$ state in ^{85}Br [7]). In ^{90}Zr, the relative single particle energy of $\pi 2p_{3/2}$ with respect to $\pi 1f_{5/2}$ is not much larger than 500 keV. Additional mean-field effects probably contribute to the evolution of the relative energy of $\pi 2p_{3/2}$ and $\pi 1f_{5/2}$ between ^{78}Ni and ^{90}Zr.

The same strong monopole proton-neutron interaction with the neutrons in the $\nu 1g_{9/2}$ orbital can be expected to affect the $\pi 1g_{9/2}$ single-particle state [41]. Since there is evidence of a monopole shift in the energy of $\pi 1f_{5/2}$ relative to $\pi 2p_{3/2}$ when $\nu 1g_{9/2}$ fills, we might expect a significant monopole shift for $\pi 1g_{9/2}$ as well. The experimental data from which

the single-particle energy of the orbital $\pi 1g_{9/2}$ can be extracted are unfortunately not as clear as for the case of $\pi 1f_{5/2}$.

The lowest-energy level assigned $(9/2^+)$ in ^{69}Cu (at 2551 keV [2,22,34]) and ^{71}Cu (at 1786 keV [20,22]), should have a significant $\pi 1g_{9/2}$ component. The (M2) decay of the $(9/2^+)$ state at 1786 keV in ^{71}Cu to the first excited state assigned $(5/2^-)$ is puzzling, since an E1 decay to any of the two low-lying $(7/2^-)$ states should be favored (see Fig. 6(b)). The $\gamma-$decay mode of the state at 1786 keV is more consistent with a $9/2^+$–$7/2^-$ or $9/2^-$–$5/2^-$ combination, while the population of the states in $\beta-$decay [31] is consistent either with a $9/2^+$–$5/2^-$, or a $9/2^+$–$7/2^-$ combination. Lacking additional information on the multipolarities of the observed transitions, we adopt for the remaining discussion the spin-parity assignments of $9/2^+$ for the state at 1786 keV and $5/2^-$ for the first excited state [20,22]. From these experimental data, the excitation energy of the $(9/2_1^+)$ state decreases by ~800 keV between ^{69}Cu and ^{71}Cu, similar to the effect noted for the $5/2_1^-$ state. The particle-core model calculations for ^{69}Cu and ^{71}Cu set the single-particle energy of $\pi 1g_{9/2}$ (relative to $\pi 2p_{3/2}$) at 3.4 MeV in ^{69}Cu and 2.15 MeV in ^{71}Cu. The magnitude of the monopole shift is larger than for $\pi 1f_{5/2}$, as might be expected from the larger radial overlap of the two $1g$ orbitals compared to that for $1g$ and $1f$ [41]. If we identify, very tentatively, the state at 1489 keV in ^{73}Cu with the calculated $9/2_1^+$ state, the extracted single-particle energy of $\pi 1g_{9/2}$ will further drop to 1.65 MeV. A linear extrapolation for the position of $\pi 1g_{9/2}$ will place it at around 2 MeV above $\pi 1f_{5/2}$ in ^{78}Ni, close to the extrapolated position of $\pi 2p_{3/2}$ and probably below $\pi 2p_{1/2}$. The existence of the Z=40 subshell closure in ^{90}Zr points out again that additional mean-field effects are responsible for the evolution of the single-particle structure between ^{68}Ni and ^{78}Ni, as well as between ^{78}Ni and ^{90}Zr. The behavior of the experimental $5/2^-$ and $9/2^+$ states, the single-particle energies of the orbitals $\nu 1f_{5/2}$ and $\nu 1g_{9/2}$, as well as the linear extrapolation to ^{78}Ni, are summarized in Fig. 10(a). We show for comparison in Fig. 10(b) the calculated single-particle levels of ^{79}Cu from different shell-model calculations [22,42,43].

Another configuration whose energy seems strongly affected by the filling of the $\nu 1g_{9/2}$

orbital is the proton 2p-1h excitation across the gap at Z=28, with the proton in $\pi 1f_{7/2}^{-1}$. The energy lowering inferred from the data on ^{67}Cu, ^{69}Cu and ^{71}Cu is around 700 keV per pair of neutrons. The position of this excitation in ^{73}Cu could not be determined unambiguously from the experimental data. Similar excitations across the Z=28 gap should exist in the even-even Ni, Zn and Fe isotopes. The corresponding 2p-2h, 4p-2h and 2p-4h configurations, respectively, should be affected by an energy lowering similar to that of the 2p-1h excitations in the Cu isotopes. In this case, the configurations involving 2p-2h excitations across Z=28 might come close to the ground-state (possibly even replacing it), for neutron numbers in the immediate vicinity of N=40. Such a dramatic effect has been observed in the Zr isotopes, where the blocked collectivity between ^{90}Zr and ^{96}Zr, due to the existence of a subshell at N=56, develops over only two isotopes to a well-deformed ground-state in ^{100}Zr [44]. In the Ni isotopes beyond ^{68}Ni, however, the current experimental data do not substantiate such an effect. A deformed configuration has been predicted by Girod et al. [24] for the 0_2^+ state of ^{68}Ni. The calculated energy and half life of the deformed 0^+ state are in good agreement with those of the experimental 0_2^+ level. However, no excited band built on the 0_2^+ state of ^{68}Ni has been observed.

IV. CONCLUSIONS

The properties of several nuclei in the region of ^{68}Ni have been studied in the framework of the particle-core coupling model. The calculations suggest that ^{68}Ni is the dominant core for the adjacent odd-mass Ni and Cu nuclei. From the PCM studies, the neutron and proton single-particle energies around N=40, Z=28 have been extracted and the neutron subshell gap at N=40 was estimated to be around 3 MeV. The gap is very similar to that found in the proton single-particle spectrum at Z=40, N=50. The observed "monopole shift" of the proton orbitals $\pi 1f_{5/2}$, and possibly also $\pi 1g_{9/2}$, takes place after N=40 is crossed. This is a strong argument for a nearly zero occupancy of $\nu 1g_{9/2}$ before N=40, indicating a significant subshell closure. These findings, in addition to the behavior of the

empirical quantities $E(2_1^+)$, differential neutron separation energies, and pairing gap in the Ni isotopes, are consistent with a good subshell closure at N=40. The possibility that multi-particle, multi-hole excitations may play a role in the low-energy structure of nuclei around ^{78}Ni has been suggested.

V. ACKNOWLEDGEMENTS

We are grateful for valuable discussions with K. Heyde. We thank W.F. Mueller and H. Grawe for stimulating discussions, and H. Grawe for making known to us experimental results prior to publication. This work was supported in part by the National Science Foundation Grant No. PHY95-28844.

REFERENCES

[1] Ch. Engelmann, F. Ameil, P. Armbruster, M. Bernas, S. Czajkowski, Ph. Dessagne, C. Donzaud, H. Geissel, A. Heinz, Z. Janas, C. Kozhuharov, Ch. Miehe, G. Münzenberg, M. Pfützner, C. Rohl, W. Schwab, C. Stephan, K. Summerer and L. Tassan-Got, B. Voss, Z. Phys. **A352**, 351(1995).

[2] R. Grzywacz, R. Beraud, C. Borcea, A. Emsallem, M. Glogowski, H. Grawe, D. Guillemaud-Mueller, M. Hjorth-Jensen, M. Houry, M. Lewitowicz, A.C. Mueller, A. Nowak, A. Plochocki, M. Pfutzner, K. Rykaczewski, M.G. Saint-Laurent, J.E. Sauvestre, M. Schaefer, O. Sorlin, J. Szerypo, W. Trinder, S. Viteritti and J. Winfield, Phys. Rev. Lett. **81**, 766 (1998).

[3] M. Bernas, Ph. Dessagne, M. Langevin, J. Payet, F. Pougheon, P. Roussel, Phys. Lett. **113B**, 279 (1982).

[4] R. Broda, B. Fornal, W. Krolas, T. Pawlat, D. Bazzacco, S. Lunardi, C. Rossi-Alvarez, R. Menegazzo, G. de Angelis, P. Bednarczyk, J. Rico, D. De Acuna, P.J. Daly, R.H. Mayer, M. Sferrazza, H. Grawe, K.H. Maier and R. Schubart , Phys. Rev. Lett. **74**, 868 (1995).

[5] J. Dobaczewski, I. Hamamoto, W. Nazarewicz and J.A. Sheikh, Phys. Rev. Lett. **72**, 981 (1994).

[6] M. Hannawald, T. Kautzsch, A. Wöhr, W.B. Walters, K.-L. Kratz, V.N. Fedoseyev, V.I. Mishin, W. Bohmer, B. Pfeiffer, V. Sebastian, Y. Jading, U. Koster, J. Lettry, H.L. Ravn, and the ISOLDE Collaboration, Phys. Rev. Lett. **82**, 1391 (1999).

[7] *Table of Isotopes, 8th edition* Vol. I, ed. R.B. Firestone (John Wiley & Sons, New York, 1996).

[8] G. Audi and A.H. Wapstra, Nucl. Phys. **A595**, 409 (1995).

[9] A. Bohr and B. Mottelson, *Nuclear Structure* Vol. I, (W. A. Benjamin Inc., London, 1969).

[10] K. Heyde and P. J. Brusaard, Nucl. Phys. **A104**, 81(1967).

[11] K. Heyde, *The Nuclear Shell Model* (Springer-Verlag, Berlin, 1994).

[12] L. Trache, K. Heyde and P. von Brentano. Nucl. Phys. **A554**, 118 (1993).

[13] K. Heyde, P. Van Isacker, M. Waroquier, J.L. Wood and R.A. Meyer, Phys. Rep. **102** (1983).

[14] G. Mairle, M. Seeger, M. Ermer, P. Grabmayr, A. Mondry and G.J. Wagner, Nucl. Phys. **A543**, 558 (1992).

[15] G. Mairle, M. Seeger, M. Ermer, P. Grabmayr, A. Mondry and G.J. Wagner, Phys. Rev. **C47**, 2113 (1993).

[16] A. Bohr and B. Mottelson, *Nuclear Structure* vol. II, W. A. Benjamin Inc., London, Amsterdam, 1975.

[17] J. Dudek, Z. Szymanski and T. Werner, Phys. Rev. **C23**, 920 (1981).

[18] J.E.Koops and P.W.M.Glaudemans, Z.Phys. **A280**, 181 (1977).

[19] T. Pawlat, R. Broda, W. Krolas, A. Maj, M. Zieblinski, H. Grawe, R. Schubart, K.H. Maier, J. Heese, H. Kluge and M. Schramm, Nucl. Phys. **A574**, 623 (1994).

[20] T. Ishii, M. Asai, I. Hossain, P. Kleinheinz, M. Ogawa, A. Makishima,S. Ichikawa, M. Itoh, M. Ishii and J. Blomqvist, Phys. Rev. Lett. **81**, 4100 (1998).

[21] J.A. Winger, J.C. Hill, F.K. Wohn, E.K. Warburton, R.L. Gill, A. Piotrowski, R.B. Schuhmann, D.S. Brenner, Phys.Rev. **C42**, 956 (1990).

[22] H. Grawe, M. Gorska, Z. Hu, E. Roeckl, M. Lipoglavsek, C. Fahlander, J. Nyberg, R. Grzywacz, K. Rykaczewski, J.M. Daugas and M. Lewitowicz, GSI-Preprint-99-16, May

1999; H. Grawe, priv. comm., June 1999.

[23] W.F. Mueller, B. Bruyneel, S. Franchoo, H. Grawe, M. Huyse, U. Koster, K.-L. Kratz, K. Kruglov, Y. Kudryavtsev, B. Pfeiffer, R. Raabe, I. Reusen, P. Thirolf, P. Van Duppen, J. Van Roosbroeck, L. Vermeeren, W. B. Walters, and L. Weissman, Phys. Rev. Lett. **83**, 3613(1999).

[24] M. Girod, Ph. Dessagne, M. Bernas, M. Langevin, F. Pougheon and P. Roussel, Phys. Rev. **C37**, 2600 (1988).

[25] M. Bernas, Ph. Dessagne, M. Langevin, J. Payet, F. Pougheon, P. Roussel,W.-D. Schmidt-Ott, P. Tidemand-Petersson and M. Girod, Nucl. Phys. **A413**, 363 (1984).

[26] L. Weissman, A. Andreyev, B. Bruyneel, S. Franchoo, M. Huyse, K. Kruglov, Y. Kudryavtsev, W.F. Mueller, R. Raabe, I. Reusen, P. Van Duppen, J.Van Roosbroeck, L. Vermeeren, U. Koster, K.L. Kratz, B. Pfeiffer, P. Thirolf, and W.B. Walters , Phys. Rev.**C59**, 2004 (1999).

[27] U. Bosch, W.-D. Schmidt-Ott, E. Runte, P. Tidemand-Petersson, P. Koschel, F. Meissner, R. Kirchner, O. Klepper, E. Roeckl, K. Rykaczewski, and D. Schardt, Nucl. Phys. **A477**, 89 (1988).

[28] P.H. Dessagne, M. Bernas, M. Langevin, G.C. Morrison, J. Payet, F. Pougheon and P. Roussel, Nucl. Phys. **A426**, 399 (1984).

[29] U. Bosch, W.-D.Schmidt-Ott, P.Tidemand-Petersson, E. Runte, W. Hillebrandt, M. Lechle, F.-K. Thielemann, R. Kirchner, O. Klepper, E. Roeckl, K. Rykaczewski, D. Schardt, N. Kaffrell, M. Bernas, Ph. Dessagne, and W. Kurcewicz, Phys. Lett. **164B**, 22 (1985).

[30] J.I. Prisciandaro, P.F. Mantica, A.M. Oros-Peusquens, D.W. Anthony, M. Huhta, P.A. Lofy, and R.M. Ronningen, Phys. Rev. **C60**, 054307 (1999).

[31] S. Franchoo, M. Huyse, K. Kruglov, Y. Kudryavtsev, W.F. Mueller, R. Raabe, I. Reusen, P. Van Duppen, J. Van Roosbroeck, L. Vermeeren, A. Wöhr, K.-L. Kratz, B. Pfeiffer, and W.B. Walters, Phys. Rev. Lett. **81**, 3100 (1998); S. Franchoo, Ph.D. Thesis, Leuven 1999, unpublished.

[32] M. Eschenauer, A.M. Oros, E. Radermacher, M. Wilhelm, S. Albers, M. Luig, P. von Brentano, G. Graw, B. Valnion, and A. Gollwitzer, J. Phys.(London) **G22**, L51 (1996).

[33] P. Van Isacker, K. Heyde, M. Waroquier and H. Vincx, Phys. Rev. **C19**, 498(1979).

[34] T. Ishii, M. Asai, A. Makishima, I. Hossain, M. Ogawa, J. Hasegawa, M. Matsuda and S. Ichikawa, contribution to the conference "Experimental Nuclear Physics in Europe - Facing the next millennium", June 21 - 26 1999, Sevilla, Spain.

[35] B.Zeidman and J.A.Nolen, Jr., Phys. Rev. **C18**, 2122 (1978).

[36] F. Ajzenberg-Selove, R.E. Brown, E.R. Flynn and J.W. Sunier, Phys. Rev. **C24**, 1762 (1981).

[37] E.Runte, K.-L. Gippert, W.-D. Schmidt-Ott, P. Tidemand-Petersson, L. Ziegeler, R. Kirchner, O. Klepper, P.O. Larsson, E. Roeckl, D. Schardt, N. Kaffrell, P. Peuser, M. Bernas, P. Dessagne, M. Langevin, and K. Rykaczewski, Nucl. Phys. **A441**, 237 (1985).

[38] T. Ishii, M. Itoh, M. Ishii, A. Makishima, M. Ogawa, I. Hossain, T.Hayakawa, T.Kohno, Nucl. Instrum. Methods Phys. Res. **A395**, 210 (1997).

[39] L. Trache, A. Kolomiets, S. Shlomo, K. Heyde, H. Dejbakhsh, C.A. Gagliardi, R.E. Tribble, X.G. Zhou, V.E. Iacob and A.M. Oros, Phys.Rev. **C54**, 2361 (1996).

[40] J. Duflo and A.P. Zuker, Phys. Rev. **C59**, R2347 (1999).

[41] K. Heyde, J. Jolie, J. Moreau, J. Ryckebusch, M. Waroquier, P. van Duppen, M. Huyse, J.L. Wood, Nucl. Phys. **A466**, 189 (1987).

[42] J. Sinatkas, L.D. Skouras, D. Strottman, J.D. Vergados, J. Phys. (London) **G18**, 1377

(1992).

[43] X. Ji and B.H. Wildenthal, Phys. Rev. **C37**, 1256 (1988).

[44] J.L. Wood, K. Heyde, W. Nazarewicz, M. Huyse and P. Van Duppen, Phys. Rep. **215**, 101 (1992).

TABLES

TABLE I. Energies of the phonons and the dimensionless particle-vibration coupling strengths ξ_2 and ξ_3 used in the PCM calculations for each core. Also listed are the unperturbed energy of the lowest 2p-1h or 2h-1p excitation and the quadrupole moments of the phonons. The values given in parenthesis represent either extrapolated values, or were determined from states with tentative assignments.

Parameters	^{67}Ni	^{69}Ni	^{65}Cu	^{67}Cu	^{69}Cu	^{71}Cu	^{73}Cu
$\hbar\omega_2(1)$ (MeV)	2.034	2.034	1.545	1.425	2.034	1.259	(1.200)
$\hbar\omega_2(2)$ (MeV)	1.424	1.259	1.039	1.077	0.884	0.652	0.605
$\xi_2(1)$	0.8	0.8	1.6	1.5	0.8	1.4	(1.4)
$\xi_2(2)$	1.6	1.4	2.0	2.0	2.1	2.2	(2.3)
$\hbar\omega_3(1)$ (MeV)	(3.200)	(3.200)	3.560	3.371	(3.200)	(3.100)	(3.100)
$\hbar\omega_3(2)$ (MeV)	3.371	(3.100)	2.826	2.750	2.859	(2.800)	(2.700)
$\xi_3(1)$	1.4	1.4	1.3	1.4	1.4	1.4	(1.4)
$\xi_3(2)$	1.3	1.4	1.6	1.7	1.6	1.6	(1.6)
ϵ(2p-1h) or ϵ(2h-1p)	1.63	0.45	1.95	1.85	1.65	0.75	(0.70)
$Q(2^+)(fm^2)$	-15	-15	+15	+20	-15	-25	(-25)
$Q(3^-)(fm^2)$	+15	+15	+20	+20	+15	-30	(-30)

TABLE II. Neutron and proton single-particle energies used in the PCM calculations. The best-fit values are determined within ~100 keV. The values given in parenthesis represent either extrapolated values, or were determined from states with tentative assignments.

	Nucleus	$\epsilon(2p_{3/2})$ [MeV]	$\epsilon(1f_{5/2})$ [MeV]	$\epsilon(2p_{1/2})$ [MeV]	$\epsilon(1g_{9/2})$ [MeV]	$\epsilon(1f_{7/2})$ [MeV]	$\epsilon(2s_{1/2})$ [MeV]	$\epsilon(1d_{3/2})$ [MeV]	$\epsilon(1d_{5/2})$ [MeV]
ν	^{67}Ni	2.0	0.45	0.0	0.0				
	^{69}Ni	2.0	0.45	0.0	0.0				
π	^{65}Cu	0.0	0.90	1.20	3.30	0.0			
	^{67}Cu	0.0	0.90	1.30	3.30	0.0			
	^{69}Cu	0.0	0.90	1.30	3.40	0.0			
	^{71}Cu	0.0	0.25	(1.25)	2.15	0.0			
	^{73}Cu	0.0	-0.30	(1.25)	1.65	0.0			
	^{63}Co	0.0	1.00	1.10	3.30	0.0	3.70	4.0	10.0

TABLE III. Calculated and experimental branching ratios for the decay of the 2p-1h "quasi-band" in ^{69}Cu. The experimental values are taken from Refs. [31,34]. A value of B(E2)=600 e^2fm^4 has been used for the E2 transition $0_1^+ \rightarrow 2_1^+$ in ^{68}Ni and a values of B(E2)=2000 e^2fm^4 for the $0_1^+ \rightarrow 2_1^+$ transition in ^{70}Zn [7]. The collective value $|g_R| = Z/A$ has been used for the core gyromagnetic factors. The proton single-particle effective charge for E2 transitions equals 1.0, and the effective proton gyromagnetic factor of $0.66 g_{\rm free}$.

J_i^π	E_i(exp.) [keV]	J_f^π	E_f(exp.) [keV]	E_γ(exp.) [keV]	I_{rel}(exp.) %	E_i(calc.) [keV]	E_f(calc.) [keV]	B(E2) e^2 fm^4	B(M1) μ_N^2	I_{rel}(calc.) %
$13/2^-$	3214	$11/2^-$	2667	546	100	3218	2676	400	1.36	100
		$9/2^-$	2181	1033	29	3218	2235	552	–	20
$11/2^-$	2667	$9/2^-$	2181	486	100	2676	2235	339	1.39	100
		$7/2^-$	1711	957	9	2676	1624	406	–	14
$9/2^-$	2181	$7/2^-$	1711	470	100	2235	1624	526	0.47	100
		$5/2^-$	1213	–	–	2235	1161	0.11	–	10^{-4}

FIGURES

FIG. 1. Systematic behavior of the excitation energy of the first 2^+ state in the even Ni (Z=28), Zn (Z=30) and Fe (Z=26) isotopes. The neutron shell- and subshell-closures at N=28 and N=40 are indicated. The data are taken from Refs. [2], [6] and [7].

FIG. 2. (a) Differential two-neutron separation energies in the Ni isotopes, $S_{2n}(A)$-$S_{2n}(A+2)$. (b) Similar for the two-proton separation energies in the N=50 isotones. The data are taken from the evaluation of Ref. [8].

FIG. 3. Experimental neutron pairing gap in the Ni isotopes (open diamonds), calculated with the method given in Ref. [9]. The pairing gap obtained in a standard BCS approach is plotted as filled circles. The nuclear masses are taken from the evaluation of Ref. [8].

FIG. 4. Experimental and calculated states in ^{67}Ni and ^{69}Ni. Selected states (experimental and extrapolated) in the core ^{68}Ni are shown in the middle part of the figure. The experimental levels are taken from Refs. [2,7,23,26,30].

FIG. 5. Calculated fragmentation of 1h and 2h-1p strength in ^{67}Ni and ^{69}Ni. We show states with single-particle(hole) components including the hole orbitals $2p^{-1}_{1/2}, 1f^{-1}_{5/2}, 2p^{-1}_{3/2}, 1f^{-1}_{7/2}$ and the particle orbital $1g_{9/2}$.

FIG. 6. Calculated and experimental levels for (a) ^{69}Cu, (b)^{71}Cu and (c) ^{73}Cu. The experimental levels are taken from Refs. [7,22,31,34] for ^{69}Cu, from Refs. [2,22] for ^{71}Cu and from Ref. [31] for ^{73}Cu. For each isotope, known isomeric states are plotted with thick lines. The calculated states suggested to correspond to the experimental levels are plotted with long lines. The remaining calculated states are plotted with short lines on the right hand side of the figure.

FIG. 7. Experimental $7/2^-$ states in the odd-mass Cu isotopes. The spectroscopic factors obtained in the one proton pick-up reaction are given where available. The states with dominant 2p-1h component are plotted with thick line. The states with dominant $2^+(\mathrm{Ni})\otimes\pi 2p_{3/2}$ structure are connected with a dotted line. The spin and structure assignments for the two levels in ^{73}Cu are tentative (see also text). The experimental levels are taken from Refs. [7,31].

FIG. 8. Calculated and experimental spectroscopic factors for states with significant proton-particle component in ^{65}Cu and ^{67}Cu. A few states, marked with an asterisk, have a single-hole component from the orbital $1f_{7/2}$. The experimental spectroscopic factors from the one-proton pick-up reactions (d,^{3}He) and (t,α) (the latter only for ^{65}Cu) have been used for these states. For all other states in ^{65}Cu, the spectroscopic factors from the stripping (^{3}He,d) and (α,t) reactions have been used. For ^{67}Cu, only data from proton pick-up reaction (d,^{3}He) are available. The experimental data are taken from Ref. [7].

FIG. 9. "Bare" single-particle energies in ^{68}Ni (left-hand side), determined from the experimental data with the particle-core coupling model. The single-particle energies for ^{56}Ni, determined with the same method in Ref. [39], are given on the right-hand side. We compare the values with predictions using the recent parametrization of the nuclear monopole hamiltonian of Ref. [40], shown in the boxes marked with an asterisk.

FIG. 10. (a) Experimental yrast $5/2^-$ and $9/2^+$ states in the odd-mass Cu isotopes and the single-particle energies of the $\pi 1f_{5/2}$ and $\pi 1g_{9/2}$ orbitals relative to the $\pi 2p_{3/2}$ orbital, extracted from the PCM calculations. A linear extrapolation of the $\pi 1f_{5/2}$ and $\pi 1g_{9/2}$ single-particle energies toward ^{78}Ni is shown. The experimental levels are taken from Refs. [22,31]. The $(9/2^+)$ level in ^{73}Cu marked with an asterisk is the very tentative assignment discussed in the text. (b) Single-particle energies in ^{79}Cu from shell-model calculations: I from Grawe et al. [22], II from Ji and Wildenthal [43], and III from Sinatkas et al. [42].

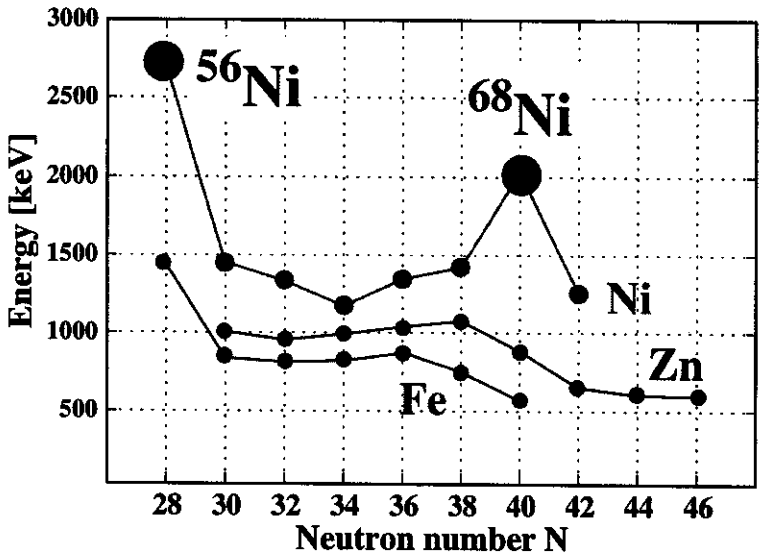
3000
2500
2000
1500
1000
500
Energy [keV]
56Ni
68Ni
Ni
Zn
Fe
28
30
32
34
36
38
40
42
44
46
Neutron number N

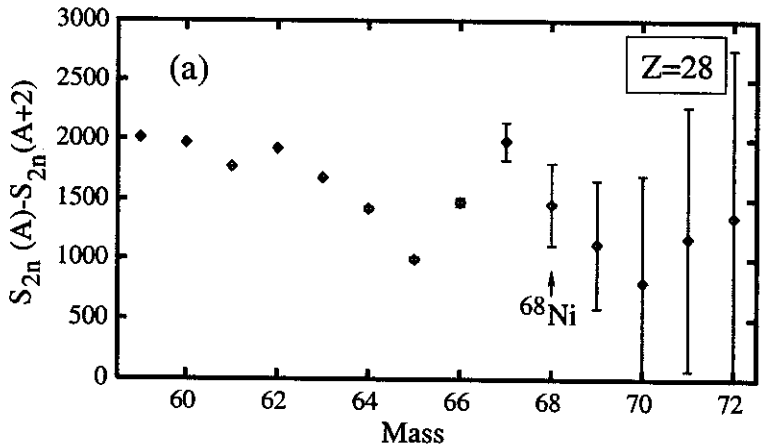
(a)
Z=28
S_{2n} (A)-S_{2n}(A+2)
^{68}Ni
Mass

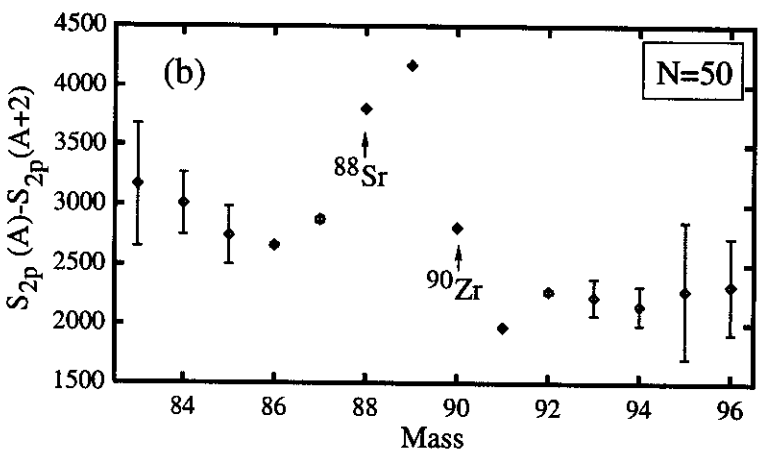
(b)
N=50
S_{2p} (A)-S_{2p}(A+2)
^{88}Sr
^{90}Zr
Mass

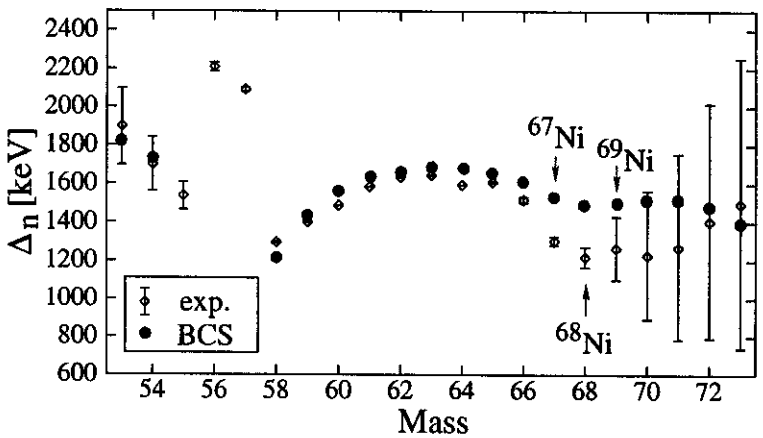
2400
2200
2000
1800
1600
1400
1200
1000
800
600
Δ_n [keV]
54
56
58
60
62
64
66
68
70
72
Mass
exp.
BCS
^{67}Ni
^{69}Ni
^{68}Ni

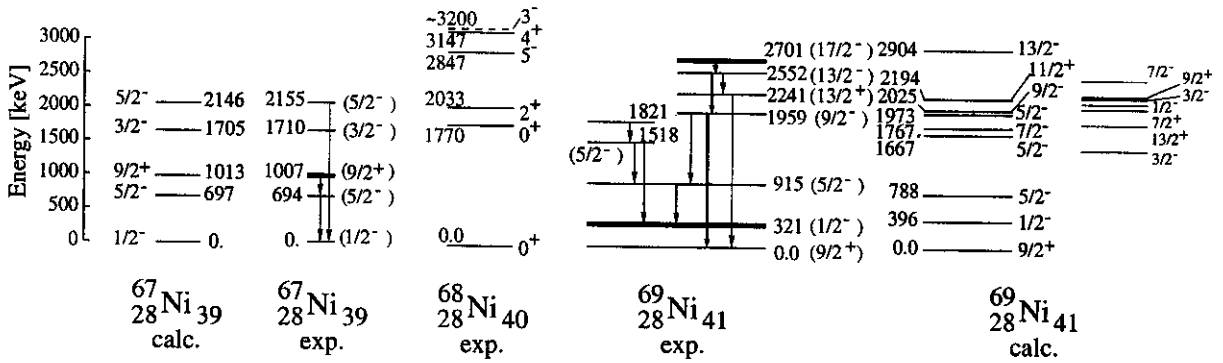
Energy [keV]
3000
2500
2000
1500
1000
500
0
5/2⁻ 2146
3/2⁻ 1705
9/2⁺ 1013
5/2⁻ 697
1/2⁻ 0.
67 28 Ni 39
calc.
2155 (5/2⁻)
1710 (3/2⁻)
1007 (9/2⁺)
694 (5/2⁻)
0. (1/2⁻)
67 28 Ni 39
exp.
~3200 3⁻
3147 4⁺
2847 5⁻
2033 2⁺
1770 0⁺
0.0 0⁺
68 28 Ni 40
exp.
2701 (17/2⁻)
2552 (13/2⁻)
2241 (13/2⁺)
1959 (9/2⁻)
1821
1518
(5/2⁻)
915 (5/2⁻)
321 (1/2⁻)
0.0 (9/2⁺)
69 28 Ni 41
exp.
2904 13/2⁻
2194 11/2⁺
2025 9/2⁻
1973 5/2⁻
1767 7/2⁻
1667 5/2⁻
788 5/2⁻
396 1/2⁻
0.0 9/2⁺
7/2⁻
9/2⁺
3/2⁻
1/2⁻
7/2⁺
13/2⁺
3/2⁻
69 28 Ni 41
calc.

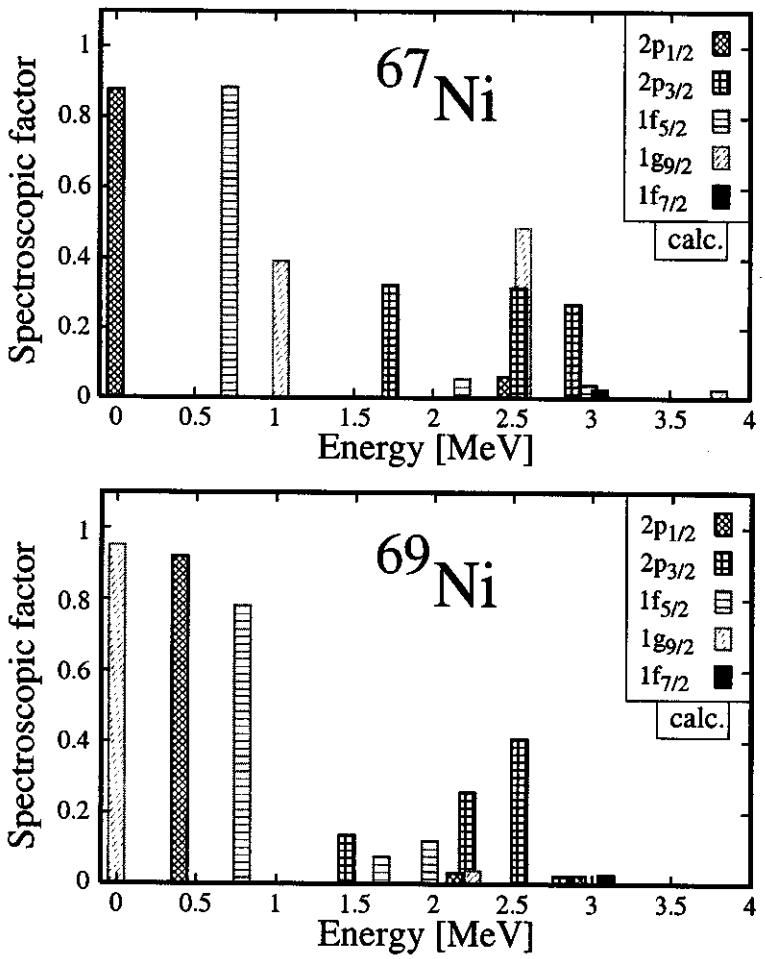
^{67}Ni
^{69}Ni
Spectroscopic factor
Energy [MeV]
$2p_{1/2}$
$2p_{3/2}$
$1f_{5/2}$
$1g_{9/2}$
$1f_{7/2}$
calc.
0
0.2
0.4
0.6
0.8
1
0.5
1.5
2
2.5
3
3.5
4

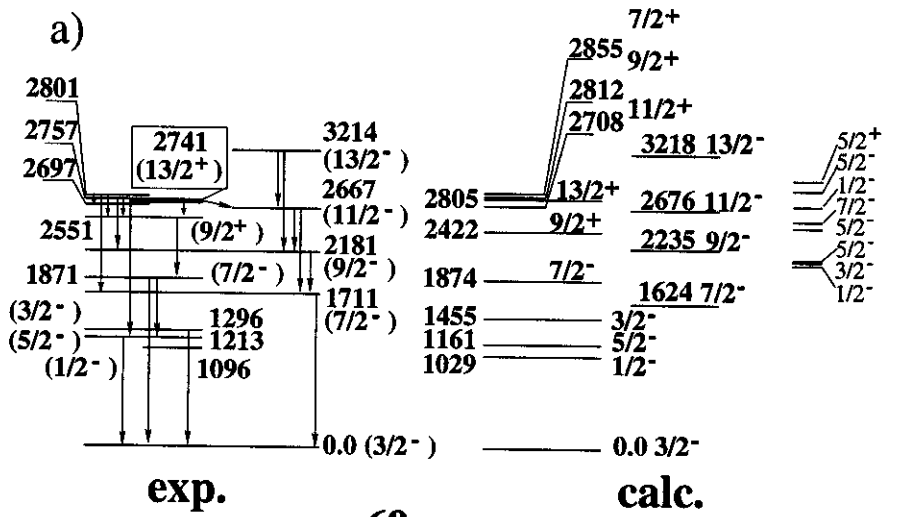

$^{69}_{29}Cu_{40}$

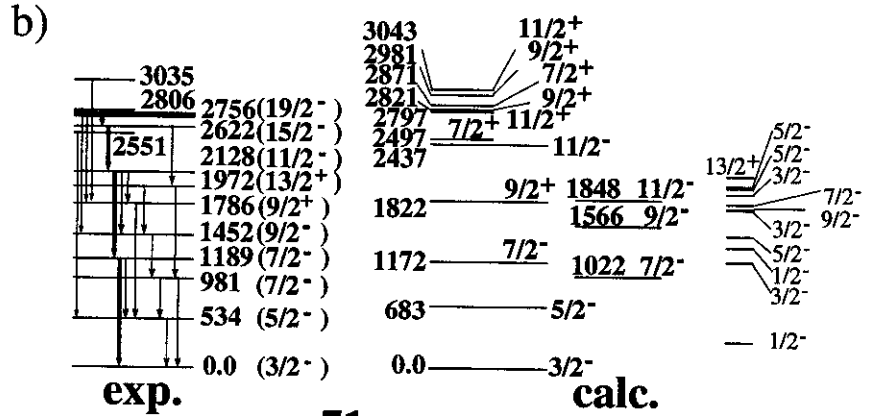

$^{71}_{29}Cu_{42}$

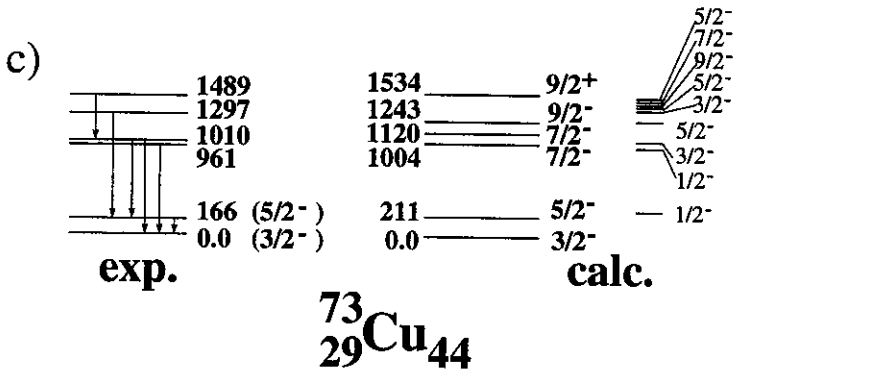

$^{73}_{29}Cu_{44}$

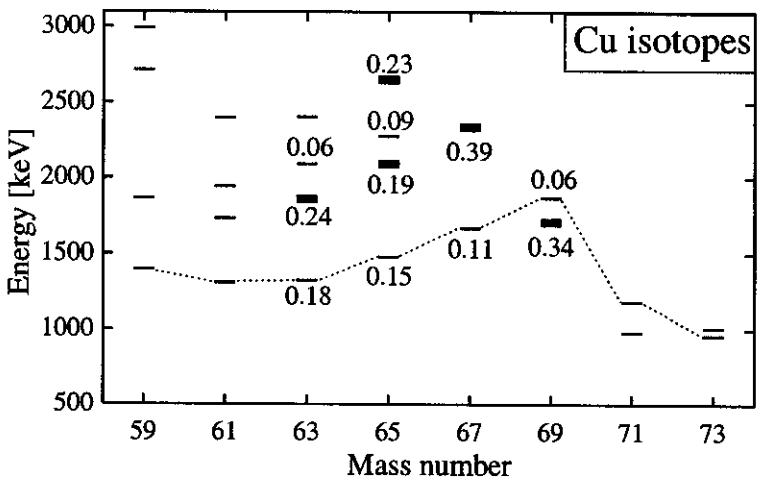
Cu isotopes
Energy [keV]
Mass number
3000
2500
2000
1500
1000
500
59
61
63
65
67
69
71
73
0.23
0.09
0.06
0.39
0.19
0.06
0.24
0.11
0.34
0.15
0.18

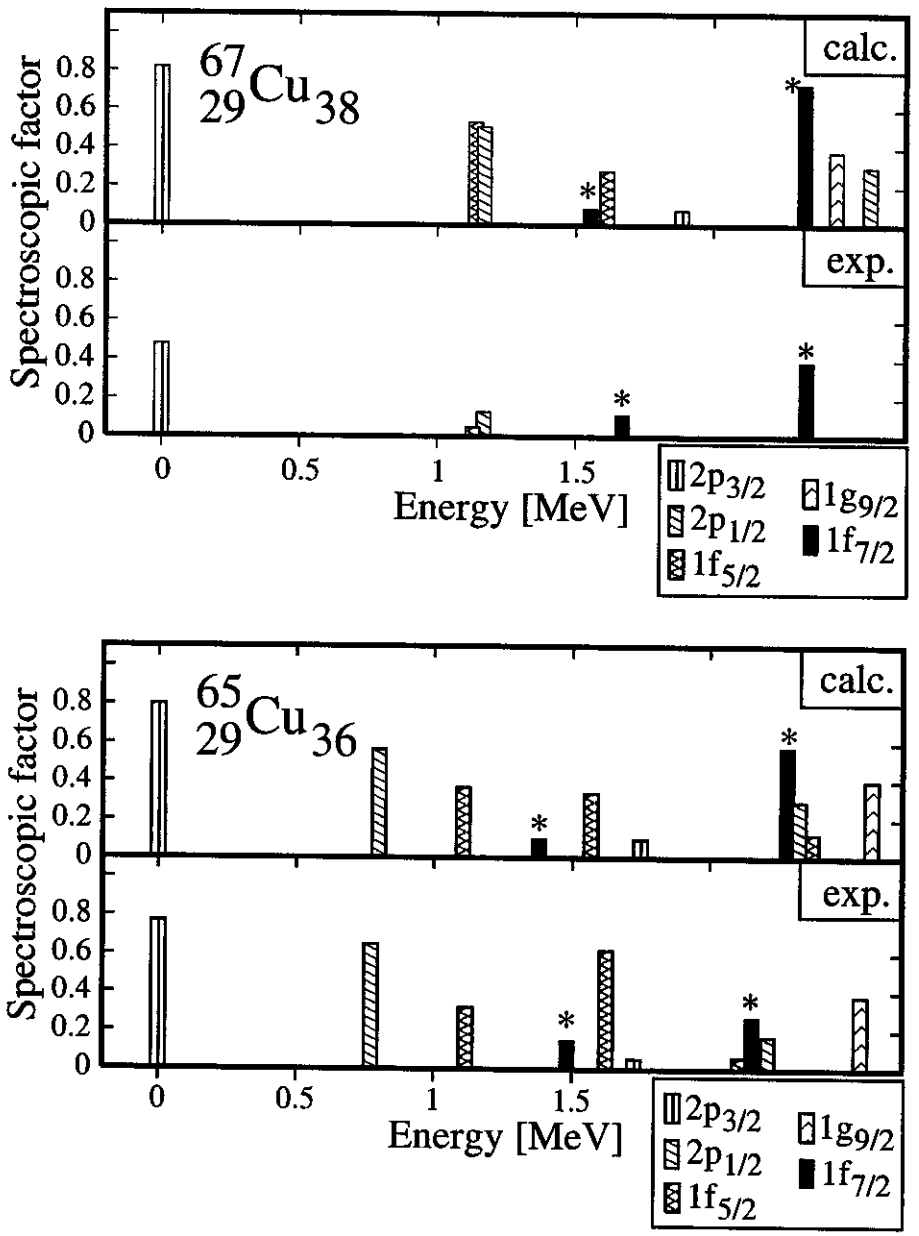
$^{67}_{29}Cu_{38}$
calc.
exp.
Spectroscopic factor
0.8
0.6
0.4
0.2
0
0
0.5
1
1.5
Energy [MeV]
$2p_{3/2}$
$2p_{1/2}$
$1f_{5/2}$
$1g_{9/2}$
$1f_{7/2}$

$^{65}_{29}Cu_{36}$
calc.
exp.
Spectroscopic factor
0.8
0.6
0.4
0.2
0
0
0.5
1
1.5
Energy [MeV]
$2p_{3/2}$
$2p_{1/2}$
$1f_{5/2}$
$1g_{9/2}$
$1f_{7/2}$

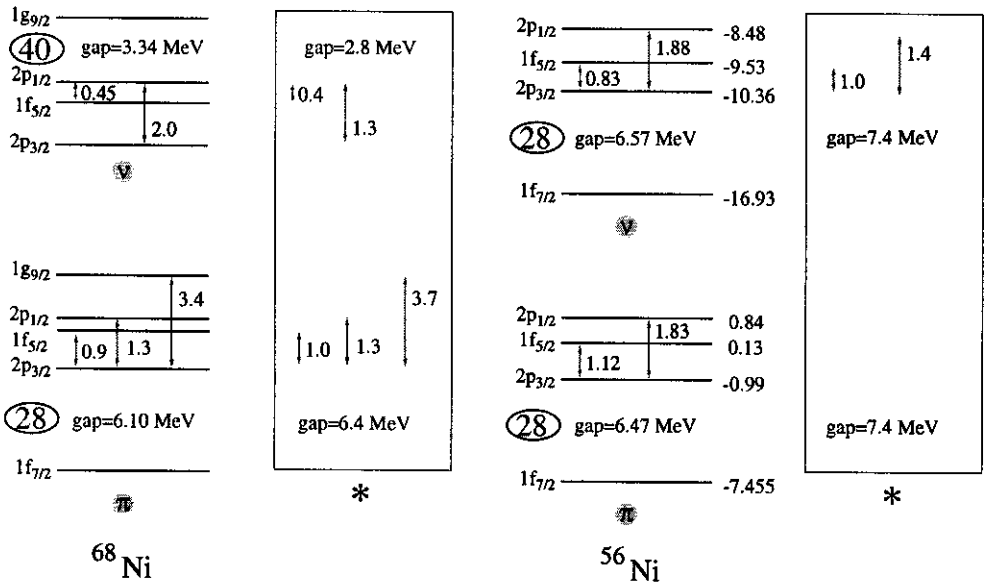
1g9/2
40
gap=3.34 MeV
2p1/2
1f5/2
2p3/2
0.45
2.0
ν
1g9/2
2p1/2
1f5/2
2p3/2
3.4
0.9
1.3
28
gap=6.10 MeV
1f7/2
π
68Ni
gap=2.8 MeV
0.4
1.3
3.7
1.0
1.3
gap=6.4 MeV
*
2p1/2
1f5/2
2p3/2
-8.48
-9.53
-10.36
1.88
0.83
28
gap=6.57 MeV
1f7/2
-16.93
ν
2p1/2
1f5/2
2p3/2
0.84
0.13
-0.99
1.83
1.12
28
gap=6.47 MeV
1f7/2
-7.455
π
56Ni
1.0
1.4
gap=7.4 MeV
gap=7.4 MeV
*

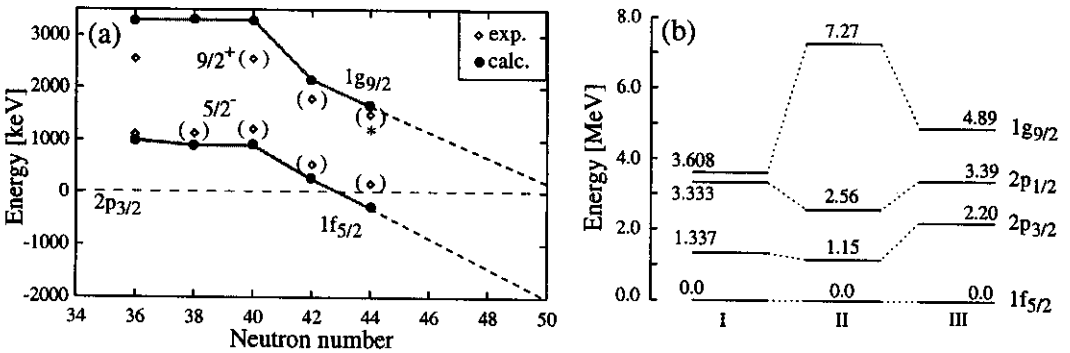
(a)
exp.
calc.
9/2+(◇)
1g9/2
5/2-
2p3/2
1f5/2
Energy [keV]
Neutron number
(b)
7.27
4.89
1g9/2
3.608
3.333
2.56
3.39
2p1/2
2.20
2p3/2
1.337
1.15
0.0
0.0
0.0
1f5/2
Energy [MeV]
I
II
III